KRYPTON IN PORE VOLUME ANALYSIS

A THESIS

Presented to

The Faculty of the Graduate Division

by

Korstiaan Van Wijngaarden

In Partial Fulfillment

of the Requirements for the Degree

Master of Science in Chemical Engineering

Georgia Institute of Technology

May 1965

In presenting the dissertation as a partial fulfillment of the requirements for an advanced degree from the Georgia Institute of Technology, I agree that the Library of the Institute shall make it available for inspection and circulation in accordance with its regulations governing materials of this type. I agree that permission to copy from, or to publish from, this dissertation may be granted by the professor under whose direction it was written, or, in his absence, by the Dean of the Graduate Division when such copying or publication is solely for scholarly purposes and does not involve potential financial gain. It is understood that any copying from, or publication of, this dissertation which involves potential financial gain will not be allowed without written permission.

3/17/65
b

KRYPTON IN PORE VOLUME ANALYSIS

Approved:

Cha

Date approved by Chairman: 5-31-65

ACKNOWLEDGMENTS

I wish to show my utmost feelings of gratitude to all the people who have given their time and assistance in order to accomplish this study. Particularly I wish to thank my thesis advisor, Dr. Clyde Orr, Jr., for his many useful suggestions and guidance throughout this investigation.

I also wish to thank the members of my reading committee, Drs. Robert A. Pierotti and J.D. Fleming, for the useful discussions I had with them and for their helpful suggestions.

Valuable assistance was rendered by Mr. Alberto Hidalgo and Mr. James McAlister, and I extend my kindest regards for their cooperation. For the most valuable assistance of all I am indebted to Mr. Bruce H. Montgomery for his continued encouragement during my program of graduate study in the U.S.A.

TABLE OF CONTENTS

LIST OF FIGURES

LIST OF TABLES

NOMENCLATURE

Symbol		Units
A_p	Surface area in pores larger than R_c	m^2/g
A	Constant	
B	Constant	
C	Constant	
K	Boltzmann constant	
L	Length of pores	m
M	Molecular weight	
P	Actual pressure	mm Hg
P_c	Critical pressure	mm Hg
P_h	Pressure during helium analyses	mm Hg
P_e	Former equilibrium pressure	mm Hg
P_s	Saturation pressure	mm Hg
R	Pore radius	A^o
R_c	Critical pore radius	A^o
R_g	Gas constant	dyne/cm mol ^oT
r_m	Radius of the meniscus	A^o
STP	Standard temperature and pressure (273^oK, 760 mm Hg)	m^2/g
S_w	Sample surface area on a weight basis	m^2/g
T_c	Critical temperature	^oK
T_{hm}	Temperature of manifold during helium analysis	^oK
T_m	Temperature of manifold	^oK
T_i	Temperature between sample space and manifold	^oK

NOMENCLATURE
(Continued)

Symbol		Units
T_s	Sample temperature	^oK
t	Film thickness	A^o
V	Volume of gas desorbed from sample	ml(STP)
V_a	Volume of gas adsorbed on sample	ml(STP)
V_c	Volume of condensed liquid in pores smaller than R_c	ml
V_f	Volume of gas evaporated from the film on the walls of partially filled pores	ml(STP)
V_i	Volume of space between sample and manifold	ml
V_m	Volume of gas evaporated from meniscus or inner capillaries	ml(STP)
V_{mo}	Manifold volume at zero pressure	ml
V_p	Total pore volume	cm^2/g
V_r	Volume of gas required to form a monolayer on the sample	ml(STP)
V_s	Volume of gas absorbed at saturation pressure	ml(STP)
V_{sa}	Sample space volume	ml
V_{sat}	True sample space volume	ml
V_{ma}	Manifold volume	ml
v	Molal volume	cm^3/mol
W_1	Weight of sample and sample tube	g
W_2	Weight of sample tube	g
W_s	Sample weight	g
σ	Surface tension	dyne cm^{-1}
ρ_a	Density of the adsorbed phase	g/cm^3

SUMMARY

Pore structures have been determined for a number of years from calculations involving low-temperature nitrogen, adsorption-desorption isotherms. Krypton, because of its low saturation pressure, offers a more satisfactory measurement than nitrogen when the pore volume is small for the same reasons that it does for surface area when the total amount of surface is limited. Unfortunately, krypton is normally a solid at liquid nitrogen temperature, that is, it is below its triple point at this temperature. However, liquid properties can be used satisfactorily in surface area calculation.

In this investigation the liquid properties of krypton at the boiling point of nitrogen were estimated and applied to a numerical integration procedure in order to calculate pore size distributions from experimentally determined desorption isotherms. The B.E.T. model of adsorption was used. Experiments and calculations were carried out with both krypton and nitrogen, using a series of samples with very different pore structures. The results show reasonable agreement for kaolin which is porous over a range of pore radii from 25 to 60 Å, this being the usable region with krypton. The agreement in the cases of boron nitrode and aluminum is also good, especially for pores above about 35 Å in radius. Here, however, the values determined may have actually been void spaces among the particles since other evidence indicates these two materials to be essentially nonporous.

Pore radii up to about 300 Å can be determined with nitrogen. The krypton analysis is limited to relative pressures, P/P_s, where P_s is the extrapolated saturation pressure of liquid krypton, of less than about 0.65, the actual value depending on the temperature. Measurement cannot be made at higher relative pressures because unlimited crystallization occurs. According to theory, pores with radii of 60 Å and smaller have then been filled, and pore size distributions only up to this radius can be calculated.

In order to avoid this limitation of krypton, while keeping most of the advantages offered by krypton, such as low saturation pressure, small molecule, inertness, and availability in a suitably pure form, ethane should be investigated as the adsorbate at -270°F.

CHAPTER I

INTRODUCTION

Definition of the Problem

The adsorption and desorption of nitrogen gas at liquid nitrogen temperature has been employed for a number of years in determining the pore structure of solids. Krypton gas because of its low saturation vapor pressure potentially offers a more satisfactory measurement than nitrogen when the pore volume is small, just as it does for surface area analysis when the total amount of surface is limited.

Measurements (at constant temperature) of the amount of a gas adsorbed V_a by a solid, when plotted as a function of the pressure, give an adsorption isotherm. The shape of such a curve gives qualitative and quantitative information about the adsorption process. Brunauer, et al.[1] show five basic isotherm shapes.

Krypton is normally a solid at liquid nitrogen temperature. However, when it is employed as the adsorbate in surface area evaluation and no more than a few molecular layers of it are allowed to form on a surface, the properties of liquid krypton can be utilized satisfactorily in the calculation. Results obtained using nitrogen and krypton are then in reasonable agreement (as shown by the results presented later).

To make a pore volume analysis, the cracks and crevices of the solid being analyzed must be filled with adsorbate. This requires the build-up

of many molecular layers and, in all likelihood, results in solid krypton as the adsorbed phase. However, Young and Crowell[2] have shown that a liquid adsorbed on the surface of a powder and reduced to a temperature below its normal freezing point might still exist as a supercooled liquid. The phase transition on the powder in any event is a gradual one, occurring at no distinct temperature. Such behavior can be derived from the phase rule. This being the case, adsorbed krypton may exist as a pure supercooled liquid, as a mixture of solid and liquid with the proportion of solid probably being dependent on location in the powder structure, or as a pure solid.

Previous tests and calculations attempting to establish the true state of adsorbed krypton have not been conclusive. Hence, experiments were undertaken in which the pore structures of several substances were evaluated by both nitrogen and krypton adsorption and desorption isotherms.

History and Methods

Pore volume analyses are important in addition to surface area data, because for many purposes the size distribution of cracks and crevices making up the internal surface area is important. For example, with catalysts the elucidation of pore structure adds much to the knowledge of catalytic activity.

Several means for pore structure determination have been developed. The simplest method would be direct measurement by means of calipers or by optical and electron microscope techniques. This, obviously, is only suitable when the materials have large pores[3]. The total volume

of pores can also be estimated by the so-called displacement method. The most suitable technique in this case is the mercury-helium method. The pore volume is determined by allowing helium to expand in a bulb containing the sample, measuring the void and pore volumes, and then measuring the volume of mercury necessary to fill the voids.[4][5] Since mercury does not fill the pores, the void volume of the system is thus evaluated and the total pore volume is obtained by differences. Pore size distribution can be measured by X-ray diffraction. It has been shown that samples of materials containing pores of colloidal proportions give a low-angle scattering pattern representative of the pores.[6][7][8] Still another method is the so-called gas flow analysis. If a material is broken into smaller and smaller parts the particle density of the pieces formed becomes progressively greater because of the elimination of pores. Densities are then evaluated from the pressure drop accompanying flow through beds of particles.[9][10]

Calculation of Pore Size Distributions from Adsorption Isotherms

The calculations are based on the assumption that the Kelvin equation

$$-R_g T \log P/P = \frac{2\sigma v}{r_m} \qquad (1)$$

is applicable. Here, R_g is the gas constant, P the vapor pressure of the liquid revealing a meniscus; P_s the vapor pressure of the bulk liquid, σ the surface tension of the condensed liquid, v the molal volume, and r_m the radius of the liquid meniscus in the capillaries involved. T is the absolute temperature. The liquid condensed in a liquid capillary

is then in equilibrium with its meniscus.

Wheeler[12] devised a theory based on this equation which took also into account the affects of multilayer adsorption. Two assumptions were made. It was first assumed that at any point on the desorption branch of the isotherm all pores larger than a certain radius R_c were covered with an adsorbed multilayer of thickness t, whereas all pores smaller than a certain radius were filled by capillary condensation. Secondly, since all unfilled pore walls have an absorbed layer of thickness t on them, it is assumed that the radius of the meniscus in a filled pore where it contacts a larger pore will not be the pore radius R_c but a smaller radius R_c-t. In other words, under conditions of adsorption, pores of true physical radius are not dealt with. Instead pores having radii effectively diminished by the thickness of the absorbed layer are treated. The maximum true pore size R_c , which will be filled at a certain relative pressure, is then given by

$$R_c = t + \frac{2\sigma v}{R_g T \log P_s/P} , \qquad (2)$$

if $(R_c - t)$ is substituted for r_m in the Kelvin equation.

Once the multilayer thickness as a function of the pressure is known, R_c may be calculated from Eq. (2). At a given pressure all pores with radii smaller than R_c will be filled with liquified adsorbate held by capillary condensation. Then assuming that thermodynamic equilibrium, as implied by the above equation, is established on the desorption branch of the isotherm, an equation for the desorption isotherm can be developed as follows: The volume V_a adsorbed at any point on the isotherm, computed as a liquid, is given by

$$V_a = V_c + V_e \ . \tag{3}$$

Here V_c is the volume of capillary condensed liquid in pores smaller than R_c and V_e is the volume of absorbed multilayers on pores larger than R_c . The pore size distribution function $L(R)dR$ is then defined as the length of all pores (per gram of adsorbent) which have radii in the range R to R+dR. The volume $V_c(R_c)$ of all pores having radii less than R_c is thus given by

$$V_c(< R_c) = \int_0^{R_c} \pi R^2 L(R)dR \ . \tag{4}$$

The surface area and pore length of pores larger than R_c are given, respectively, by:

$$A_p (> R_c) = \int_{R_c}^{S} 2\pi RL(R)dR \tag{5}$$

and

$$L(> R_c) = \int_{R_c}^{S} L(R)dR \ . \tag{6}$$

The volume of liquid condensed in capillaries, V_c, is by definition $V_c(<R_c)$ and so is connected to the pore size distribution function by Eq. (6). For a single cylindrical pore, the volume of the absorbed multilayer calculated as a liquid volume V_m is the volume of a cylindrical shell of outside radius R and inside radius R-t, or

$$\pi [R^2 - (R - t)^2] L(R)$$

or

$$\pi(2tR - t^2)\, L(R) \ .$$

Hence, the volume of gas adsorbed as a multilayer on all pores larger than R_c is the integral of this or

$$V_l = t \int_{R_c}^{S} 2\pi\, R\, L(R)\, dR = \pi t^2 \int_{R_c}^{S} L(R)\, dR \ . \qquad (7)$$

which may be written

$$V_l = t\, A_p(>R_c) - \pi t^2\, L(>R_c). \qquad (8)$$

Combining these expressions with Eq. (5) gives the following equation:

$$V_a = V_c(<R_c) + tA_p\,(>R_c) - \pi t^2\, L \ . \qquad (9)$$

The latter equation shows that the volume adsorbed at any pressure is equal to the volume condensed on the "free surface area" of capillaries not filled by capillary condensation less a correction term which takes into account the fact that pores are cylindrical. Therefore, the volume of a layer of thickness t on an area A_p is not tA_p but is smaller.

The isotherm may be written

$$V_p - V_a = \int_{R_c}^{C} \pi\, (R - t)^2\, L(R)dR \ , \qquad (10)$$

where V_g is the total pore volume per gram. If t , the multilayer thickness, is known as a function of pressure, then R_c is also known as

a function of pressure from Eq. (2).

Any of several relationships might now be used. The formula might be applied assuming for L(R) a Gaussian, a Maxwellian, or a skewed distribution. Mulligan and Adams[13] proposed an analytical expression for cumulative pore volumes and pore size distributions. Voigt and Tomlinson[14] prepared a series of distribution curves based on both spherical and cylindrical pores with Maxwellian and two types of Gaussian distributions. They described a method for fitting normalized isotherms to these curves. The solution used in this work does not require the assumption of a pore-size distribution; it employs numerical integration. Methods of this type are described by Barrett, Joyner, and Halenda[15] and by Pierce[16].

The method of Pierce is the most straightforward and a minor modification of it is employed in this work. Each increment of gas desorbed, V, is composed of the gas evaporated from the meniscus of inner capillaries, V_m, and the gas evaporated from the film on the walls of the unfilled pores V_f, i.e.,

$$V_m = V - V_f \ . \tag{11}$$

V is determined directly from the experimental isotherm and the relationship

$$V_f = \Delta t \ \Sigma A_p \ , \tag{12}$$

where A_p is the surface area of all pores not filled by capillary condensation.

For each desorption increment the pore surface area is

$$A_p = \frac{2V_p}{R_c} , \tag{13}$$

where the volume of the pores in the corresponding increment is

$$V_p = V_m \left(\frac{R_c}{R_c - t}\right)^2 . \tag{14}$$

Then the total length of the pores in this size range having a mean radius R is

$$L(R) = \frac{V_p}{\pi R_c^2} . \tag{15}$$

In these equations the mean values of R_c and t over the desorption increment should be used for greatest accuracy. In general, the smaller the increments of integration the more accurate are the results. To obtain the best results, care must be exercised in reading V_a from the absorption isotherms, and a statistical approach should be used to minimize the reading error.

If the volume of gas adsorbed at STP per gram of adsorbent at the saturation pressure is V_s , then the volume of the adsorbed phase in the pore volume is

$$V_p = \frac{V_s M}{M_v \rho_a} , \tag{16}$$

where M is the molecular weight, M_v the molar volume, and ρ_a the density of the adsorbed phase. This density, in general, is believed very nearly equal to that of liquified adsorbate at the same temperature,

which is a specific gravity of 0.808[4] for liquid nitrogen at its normal boiling point.

In these calculations it was assumed that all pores are cylinders which, admittedly, is a very limiting restriction. Then if all the surface is attributed to the walls of the pores, the average pore radius is

$$R = \frac{2\,V_p}{A_p}\,, \tag{17}$$

where A_p is the surface area per gram of absorbent. Results calculated by Eq. (17) agree well with those of other methods. The method employed results in pore radii from 20 to 300 Å. For the krypton measurements there is, however, another limitation as shown in Chapter IV.

The evaluation of the thickness of the adsorbed layer as a function of the pressure may be estimated from theoretical adsorption expressions such as those of Brunauer, Emmett, and Teller (the so-called B.E.T. equation) or by means of empirical measurements on non-porous solis. Wheeler[12] recommends that the Halsey equation which for nitrogen is

$$t(\text{Å}) = 4.3 \left[\frac{5}{\ln P/P_s}\right]^{1/3}\,, \tag{18}$$

where P/P_s is the relative pressure and 4.3 Å is taken as the thickness of a monomolecular layer of adsorbed nitrogen. For krypton the equation has to be modified in view of the specific constants for this substance.

Check on Accuracy of the Isotherms

For some time satisfactory surface area results have been obtained following the B.E.T. theory with both krypton and nitrogen. A comparison between surface areas calculated with both nitrogen and krypton is, therefore, an indication of the accuracy of the experimental results.

According to the B.E.T. theory the adsorption isotherm curve may be fit by an equation of the form

$$\frac{P}{V(P_s-P)} = \frac{1}{V_r C} + \left(\frac{C-1}{V_r C}\right)\frac{P}{P_s} \quad , \tag{19}$$

where P_s is the saturation pressure of either nitrogen or krypton, V_r is the volume of the gas required to form a monolayer on the tested solid, and C is a constant. This plot is almost always linear in the region below 0.3 P/P_s and above 0.1 P/P_s and the intercept is a small positive number on the $P/V\ (P_s-P)$ axis. The slope of the line is $(C+1)/V_r C$ and the intercept is $1/V_r C$. Since C is usually a large number, the value of V_r is essentially the reciprocal of the slope of the line.

Since V_r is conveniently expressed in milliliters of adsorbate per gram of sample and since one molecule of adsorbed nitrogen gas occupies 15.8 $\mathring{A}$, the conversion from the plotted results to specific surface area is simply given by

$$S_{wN_2} = \frac{15.8 \times 6.023 \times 10^{23}}{22.414(\text{slope} + \text{intercept})} = \frac{4.25}{\text{slope} + \text{intercept}} \quad , \tag{20}$$

where S_w is the sample surface area expressed in square meters per gram and the other terms are Avogadro's number and the molecular gas volume.

By analogy, for krypton the final expression is

$$S_{wKr} = \frac{5.64}{\text{slope \& intercept}} . \qquad (21)$$

Criticism of the Method Used

The calculations and statements to be given are, in general, based on the assumption that the B.E.T. model applies. Nevertheless, a serious weakness of the B.E.T. theory, as noted by Cassel[18], using the Gibbs adsorption isotherm is that the surface tension of the adsorbed film at $P=P_s$ is negative. This arises from a total disregard of interaction forces. The B.E.T. model postulates that localized adsorption persists throughout all layers but adsorption in the nth layer must take place before the n-1 layer is filled. The result is not a series of continuous layers, but a random system of vertical molecular columns, according to Gorter and Frederikse[19]. Theimer[20] also has underlined the discontinuous character of B.E.T. absorbed films.

Also it has been pointed out that the integration constants of the Clausius-Clapeyron equation, when applied to adsorption and vapor pressure data, do not show the interrelationship demanded by B.E.T. theory. Dervichian[21] has shown, in addition, that the hypothesis that an isolated molecule on top of another yielding full energy of liquification is quite untenable and, of course, contradicts the fact that the second molecule can adsorb a third, and so on. Going back to the method of the pore distribution calculations, this can be summarized by stating that the method used involves the following assumptions:

(a) On the desorption branch of an isotherm there is thermodynamic equilibrium while the adsorption branch is not in equilibrium since supersaturation is probably necessary to fill a pore with condensed liquid.

(b) Each pore space must be connected with at least one larger pore for, otherwise, the smaller pore cannot empty at the proper pressure.

(c) The pores are cylindrical.

(d) The surface tension of the absorbed fluid is constant over the absorbed layers and the same as that of pure liquid at the working temperature.

(e) The meniscus radius is that of the inside tube formed by multilayer absorption.

The theory as used is thus questionable from several points of view, but it is the best available.and gives useful results for engineering purposes.

CHAPTER II

INSTRUMENTATION AND EQUIPMENT

Description of Apparatus

For the determination of the absorption-desorption isotherms presented in Chapter III, the Orr Surface-Area Pore-Volume Analyzer, Model MIC-103, of Numinco, Monroeville, Pennsylvania, was used.

The basic design of the apparatus is shown in the schematic drawing of Fig. 1. It consists in essence of (1) a seven-valve manifold through which are interconnected three sample holders; (2) an evacuation system consisting of a cold trap, a diffusion pump, and a mechanical forepump; (3) a sensitive pressure indicator; (4) a variable volume space; (5) two low-pressure detectors; (6) inlets for the gases; helium, nitrogen, and krypton; and (7) a manifold temperature indicator. One of the low pressure detectors is directly connected into the manifold. Its purposes are to indicate the extent to which samples have been freed from atmospheric gases and vapors and to serve as the main pressure indicator for krypton adsorption-desorption data. Built also into the system is a resetable timer and an adjustable switch to record how long a sample has been exposed to any level of reduced pressure. Another component of the apparatus indicates the temperature in the manifold. Adjustable heaters permit the powders to be elevated in temperature under vacuum to drive off atmospheric gases and vapors adhering to the powders. Fig. 2 is a photograph of the apparatus. An oxygen vapor pressure thermometer,

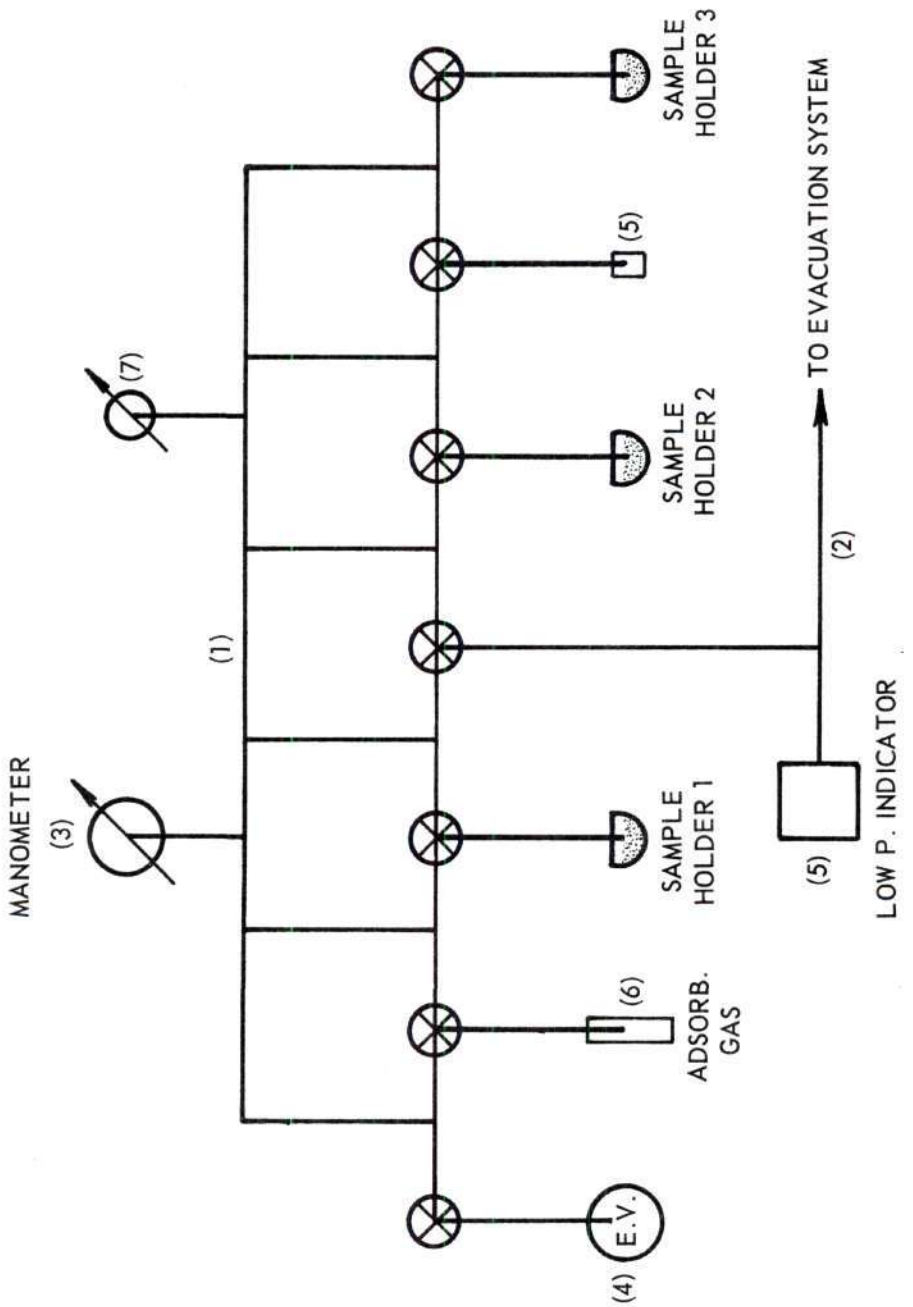

Figure 1. Schematic Diagram of Equipment.

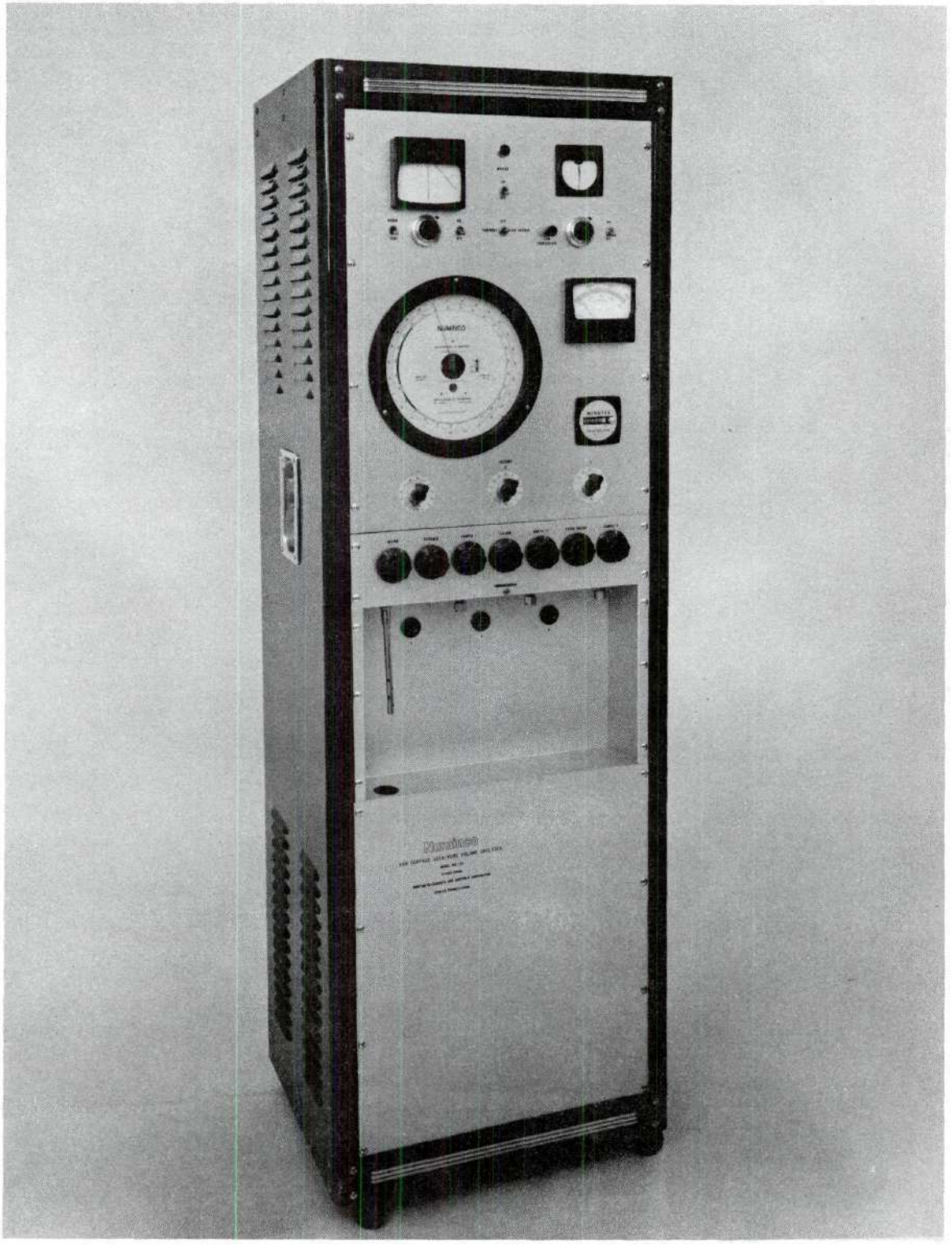

Figure 2. Photograph of Apparatus.

as shown in Fig. 3, was employed to establish accurately the liquid nitrogen's temperature; its calibration was based on data recommended by Ziegler, et al.[22].

Principle of Operation

Adsorption-desorption isotherms were obtained by measuring the volume of gas which was absorbed and then desorbed under increasing and decreasing pressures.

Start up

The instrument uses 110-120 volt AC current and draws about 750 watts. Specifically purified nitrogen, krypton, and helium gases were needed in order to determine the isotherms. These gases were supplied to a connection located in the instrument's side. The gases were supplied at pressure heads between 5 and 20 lb/in^2.

Sample Weight

A clean, dry sample tube was weighed on an analytical balance with an accuracy of 0.0001 gram. This weighing was accomplished with a small rubber stopper sealing it. The result was the weight called W_2 in Chapter III.

The amount of desired sample was next added into the sample holder. The sample holder and rubber stopper were marked with a number according to the position to which it was attached to the apparatus. The sample holder was attached to the equipment by means of a special teflon-packed holding nut, a small wad of glass wool having been placed in the neck of the holder tube to prevent the sample's escaping if the wrong valve should be opened inadvertently. The volume of the sample holders varied from

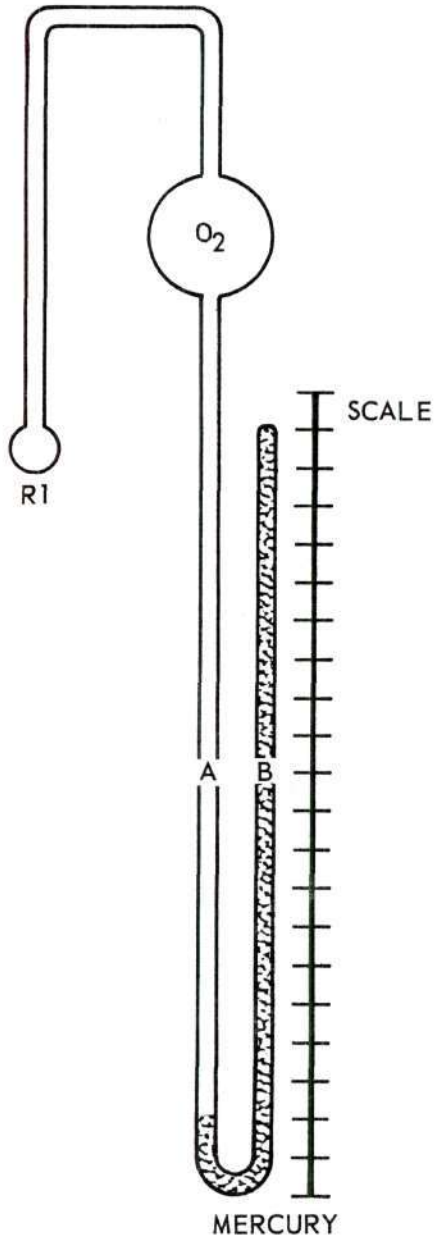

Figure 3. Oxygen Vapor Pressure Thermometer.

about 1 to 30 ml. and the weight of the samples from about 0.1 to 5 grams.

After having closed all valves, the forepump of the evacuation system was started and the pressure on the vacuum gages was noted. When the pressure dropped to 0.10 mm Hg the diffusion pump was started too. After about 5 minutes more the vacuum gage usually indicated less than 0.001 mm Hg and sometimes as low as 0.0001 mm Hg. The center vacuum valve was then opened and the system's manifold was evacuated.

Then the valve connecting the sample holder with the manifold was slowly opened and the speed of desorption was adjusted so that absorbed moisture and other gases might not boil off the sample violently. The sample's temperature was adjusted by slipping an electric heating mantel around the sample bulb and applying an adjustable voltage to it from the equipment. Because the samples involved were not subject to thermal decomposition at temperatures below 500°C, they were heated to 350°C. The higher the temperature the faster was the degassing and the cleaner, ultimately, the surface; roughly satisfactory degassing follows the relationship[2]

$$\theta = 14.4 \times 10^{4} \, t_d^{-1.77} ,$$

where θ is the time of heating in hours to the temperature t_d in degrees centigrade.

The temperature of heating was established with a thermocouple.

Degassing the Sample

Before degassing completely, but after about 10 minutes of evacuating, the vacuum valve was closed and the sample holder filled with

nitrogen. This few minutes of exposure to a high vacuum removed essentially all weighable impurities. The weight of the holder with sample was then determined on an analytical balance. This gave the weight W_1. The wad of glass wool was removed before weighing. The weight of the sample was thus given by W_1-W_2. The sample holder was filled before removal with nitrogen because it will not be appreciably adsorbed on a sample at room temperature and its presence will keep out moisture and other airborne impurities. The difference in weight between 30 ml air and 30 ml of nitrogen gas, considering even the small difference in temperature, is also negligible.

The sample holder was again attached to the apparatus, the manifold system was evacuated again, and the valve connecting the sample-holder with the manifold was opened slowly. The heaters were replaced and the heating temperature was adjusted once again. A relay switch on the vacuum gage made contact as soon as the pressure reached 5×10^{-4} mm Hg and a timing meter started.

The samples were generally degassed more than 12 hrs to a pressure as low as the apparatus was capable of achieving.

Obtaining the Unoccupied Sample Tube Volume

After degassing, the vacuum and the sample holder valve were closed and the heating mantel removed. A Dewar flask was filled with liquid nitrogen and the flask was placed about the bulb R_1 (see Fig. 3) of the oxygen-vapor thermometer. The oxygen was condensed in R_1, and the difference between the mercury column heights A and B gave the vapor pressure of pure oxygen at the temperature of the liquid nitrogen. The temperature corresponding to this vapor pressure was evaluated.

There will be a small change with time in the liquid nitrogen's temperature due to changes in atmospheric pressure and the condensation of oxygen from the air. It was found to deviate slightly.

Now a Dewar flask containing liquid nitrogen of accurately known temperature was placed around the sample to be evaluated. Helium was let into the manifold by means of the absorbate valve until the main pressure gage indicated about 500 mm Hg pressure. After allowing a minute for the sample to reach thermal equilibrium, the pressure P_{hl} was recorded. The helium temperature T_{hm} in the manifold was next recorded with the temperature indicator. The valve connecting the sample with the manifold was next opened and again time was allowed for the pressure to reach equilibrium; this usually required about 15 minutes. Since helium is a very inert gas, it is not adsorbed by the sample even at liquid nitrogen temperature, but merely fills the space in and around the sample. This pressure was noted in order to calculate the void volume of the sample holder. After this measurement, the sample was degassed again for about 15 minutes in the manner already described. The helium was thus removed from the sample.

Determination of Adsorption-Desorption Isotherms

The sample holder was immersed again in liquid nitrogen to a preestablished depth which was thereafter maintained nearly constant during the course of the experiment. This was accomplished by filling the Dewar flask at regular intervals. The vacuum and sample holder valves were closed and the absorbate left in the manifold. In the case of nitrogen the equilibrium pressure was indicated on the main pressure gage and in the case of krypton on the low pressure thermistor gage. After a few

moments for equilibration, this pressure was recorded as P_1 . For nitrogen a first-equilibrium pressure of about 200 mm Hg was sought and for krypton one of about 0.3 mm Hg. The thermistor pressure gage's range was from about 5.10^{-4} to 2.5 mm Hg. The manifold temperature was recorded as T_m just as in the procedure using helium. Then the valve connecting the sample to the system was opened and the nitrogen or krypton was admitted to the sample. Adsorption equilibrium required anywhere from 20 to 50 minutes. The equilibrium pressure was called P_2.

The steps above were repeated until in about a dozen increments the saturation P_s was reached. This was true for both nitrogen and krypton adsorption. The saturation pressure of krypton is the vapor pressure of the solid and occurs at a relative pressure, P/P_s, of 0.650 calculated from extrapolated liquid vapor pressure data. When the volume of the manifold did not permit reasonably great pressure increments, an extra volume as indicated in Fig. 1 was added to the manifold by opening the valve which connected the two.

After attaining the saturation pressure, as indicated by the fact that an additional amount of absorbate did not increase the pressure further, the process was repeated in the reverse manner. The pressure in the manifold was lowered and recorded as P_1 and then the sample holder valve was opened. The equilibrium pressure was recorded after 20 to 50 minutes as P_2.

Again in a dozen or so steps, a pressure close to 0.05 relative pressure was obtained.

By the above procedures the quantities of gas adsorbed and desorbed by a sample can be calculated because the temperature, volumes, and

pressures in all parts of the equipment were known. In effect, the calculation required accounting for the gas that is apparently missing in the system but is actually adsorbed on the sample. This is presented in Chapter III.

CHAPTER III

PROCEDURE OF CALCULATION

Adsorption and Desorption Isotherms

The volume of the instrument's manifold was fixed. A correction has, however, to be made in the volume of the pressure indicator with shifts in pressure. The quantity of the gas in the manifold was established by the relationship $P_{ma} = nRT$, where R is the gas constant. For the moment it will be assumed that, instead of an equation of state, the ideal gas law can be applied and corrected afterwards for differences in pressures calculated both with a virial equation of state up to the second coefficient and the ideal gas law at the pressure and temperature of concern. When the valve leading from the manifold to the sample was opened, the gas expanded into the new space, some of it being adsorbed by the sample. The gas is thus partly in the manifold at the apparatus temperature, partly in the sample space at liquid nitrogen temperature, partly in the tube connecting the manifold and the sample space, and partly adsorbed.

A material balance gives

$$\frac{P_1 V_{ma}}{T_m} = \frac{P_2 V_{ma}}{T_m} + \frac{P_2 V_{sa}}{T_s} + \frac{P_2 V_i}{T_i} + V_a , \qquad (22)$$

where V_{ma}, V_{sa}, and V_a are, respectively, the manifold volume, the sample space volume not occupied by the sample, and the volume adsorbed, at standard conditions (760 mm Hg and ^{o}C). V_i is the intermediate volume

between the manifold and the sample; T_m, T_s, and T_i are, respectively, the temperature of the manifold, the sample, and the intermediate space; and P_1 is the pressure under the first conditions and P_2 under the second conditions.

When the process is repeated with the next quantity of gas, the equilibrium pressure after the additional quantity is again P_2 while the initial pressure is written P_e. The volume of the gas absorbed is then expressed at standard conditions by

$$\frac{P_1 V_{ma}}{T_m} + \frac{P_1 V_{sa}}{T_s} + \frac{P_1 V_i}{T_i} = \frac{P_2 V_{ma}}{T_m} + \frac{P_2 V_{sa}}{T_s} + \frac{P_2 V_i}{T_i} + \frac{V_a\ 760}{273}. \qquad (23)$$

Several conditions must be included to make the equation exact. First, nitrogen does not behave as a perfect gas: this was corrected for up to the second virial coefficient with an equation of state expressed in in terms of P . The pressure indicator's volume changes with change in pressure may be expressed by writing V_{sat} where the sub t means that the sample volume is the true volume. The relationship becomes

$$V_{sat} = \frac{T_s}{P_2}\left[\frac{P_1(V_{mo} + mP_1) - P_2(V_{mo} + mP_2)}{T_m} - \frac{P_2 V_i}{T_i}\right], \qquad (24)$$

where V_{mo} is the manifold volume at zero pressure and m is a term expressing the increase in volume as a function of pressure. The complete material balance is then

$$\frac{P_1 V_{ma}}{T_m} + \frac{P_1 V_{sat}}{T_s}(1 + 6.6 \times 10^{-5} P_2) + \frac{P_e V_i}{T_i} =$$

$$\frac{P_2 V_{ma}}{T_m} + \frac{P_2 V_{sat}}{T_s}(1 + 6.6 \times 10^{-5} P_3) + \frac{P_2 V_i}{T_i} + \frac{760 V_a}{273}. \qquad (25)$$

The intermediate temperature T_i was taken to be given by $(T_m + T_s)/2$ since this average was applied in initial calculations of apparatus volumes.

The data were actually analyzed on a Burroughs 220 digital computer. Manual computation will be assumed, however, in order to show the method of calculation. As mentioned before, the manifold space could be enlarged by the addition of an extra volume to it. Table 1 outlines the procedure. The right column is V_a/W_s which is the total volume of gas adsorbed and P_2/P_s is the relative pressure at which the adsorption took place. The values plot so-called adsorption isotherms; the results for the two gases and three substances studied are presented as Figs. 4, 5, 6, 7, 8, and 9.

Pore Size Distribution

As with the isotherms, machine calculation was actually utilized, but hand calculation will be indicated in the following procedure. (The program for computer use is given in the Appendix.) The previously calculated desorption isotherm data from Table 1 are transferred to the first and second columns of Table 2 by writing, in the first, the relative pressure and, in the second, V_a/W_s. Columns three and four are, respectively, pore radius filled at a certain relative pressure R and the corresponding film thickness t. These numbers are specific for both nitrogen and krypton and their evaluation will be described in Chapter IV. The fifth column is the difference between successive recorded volumes. The sixth gives values in Angstrom units of the difference between the third and fourth columns. The seventh records

Table 1. Calculation Form for Adsorption and Desorption.

W_1 =____ grams T_m =____ ^{o}K P_s =____ millimeters, mercury

W_2 =____ grams T_s =____ ^{o}K A =____ = $0.3593/(T_m W_s)$

W_s =____ grams T_i =____ = $(T_m + T_s)/2$ B =____ = $\left[0.3593\ V_{st}/(T_s W_s)\right] + \left[0.3593\ V_i/(T_i W_s)\right]$

P_{h1} =____ millimeters, mercury V_{mo} =____ milliliters C =____ = $6.6B \times 10^{-5}$

P_{h2} =____ millimeters, mercury V_i =____ milliliters

m =____ V_{st} =____ milliliters = $\frac{T_s}{P_2}\left[\frac{P_1 (V_{mo} + mP_1 - P_2 (V_{mo} + mP_2)}{T_m} - \frac{P_2 V_i}{T_i}\right]$

P_1	P_2	P_e	D $P_1 - P_2$	E $V_{mo} \times D$	F $P_1^2 - P_2^2$	G m x F	H E + G	I $P_2 - P_e$	J $P_2^2 - P_e^2$	K A x H	L B x I	M C x J	V_a/W_s K-L-M	V $\Sigma (V_a/W_s)$	X P_2/P_s

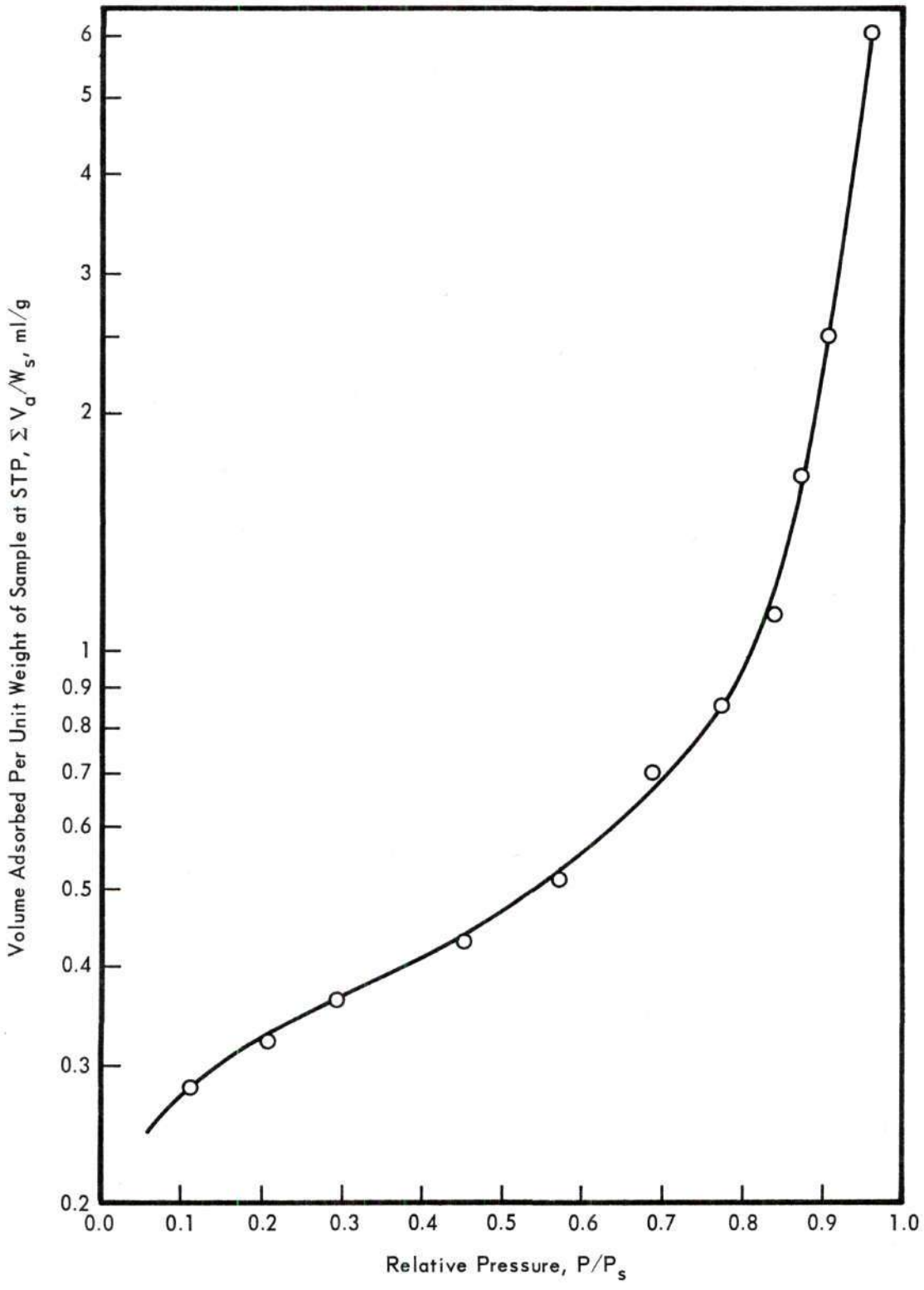

Figure 4. Nitrogen Desorption Isotherm for Aluminum Powder at 77.3 ^{o}K.

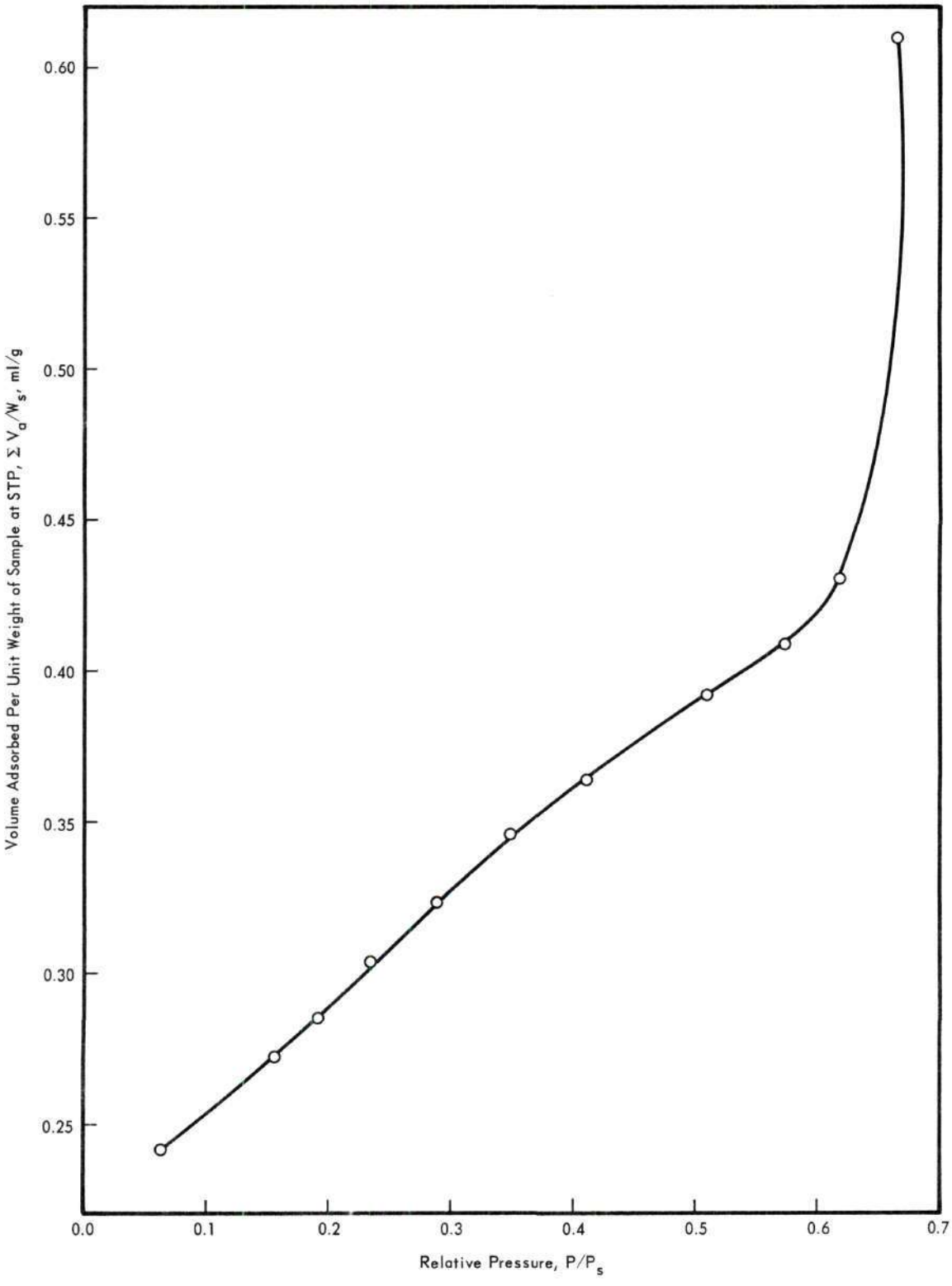

Figure 5. Krypton Desorption Isotherm for Aluminum Powder at 77.3 ^{o}K.

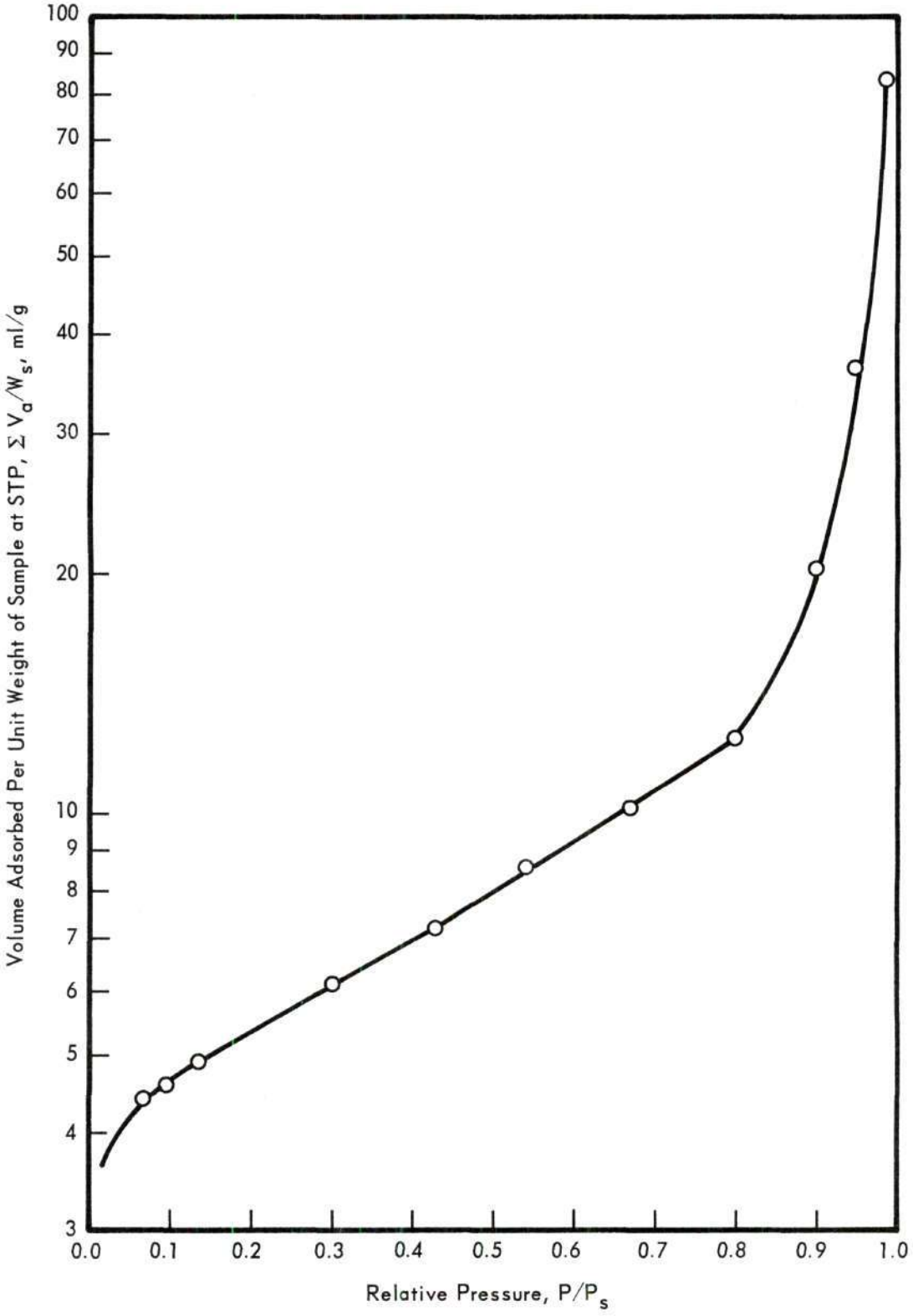

Figure 6. Nitrogen Desorption Isotherm for Boron Nitride Powder at 77.3 °K.

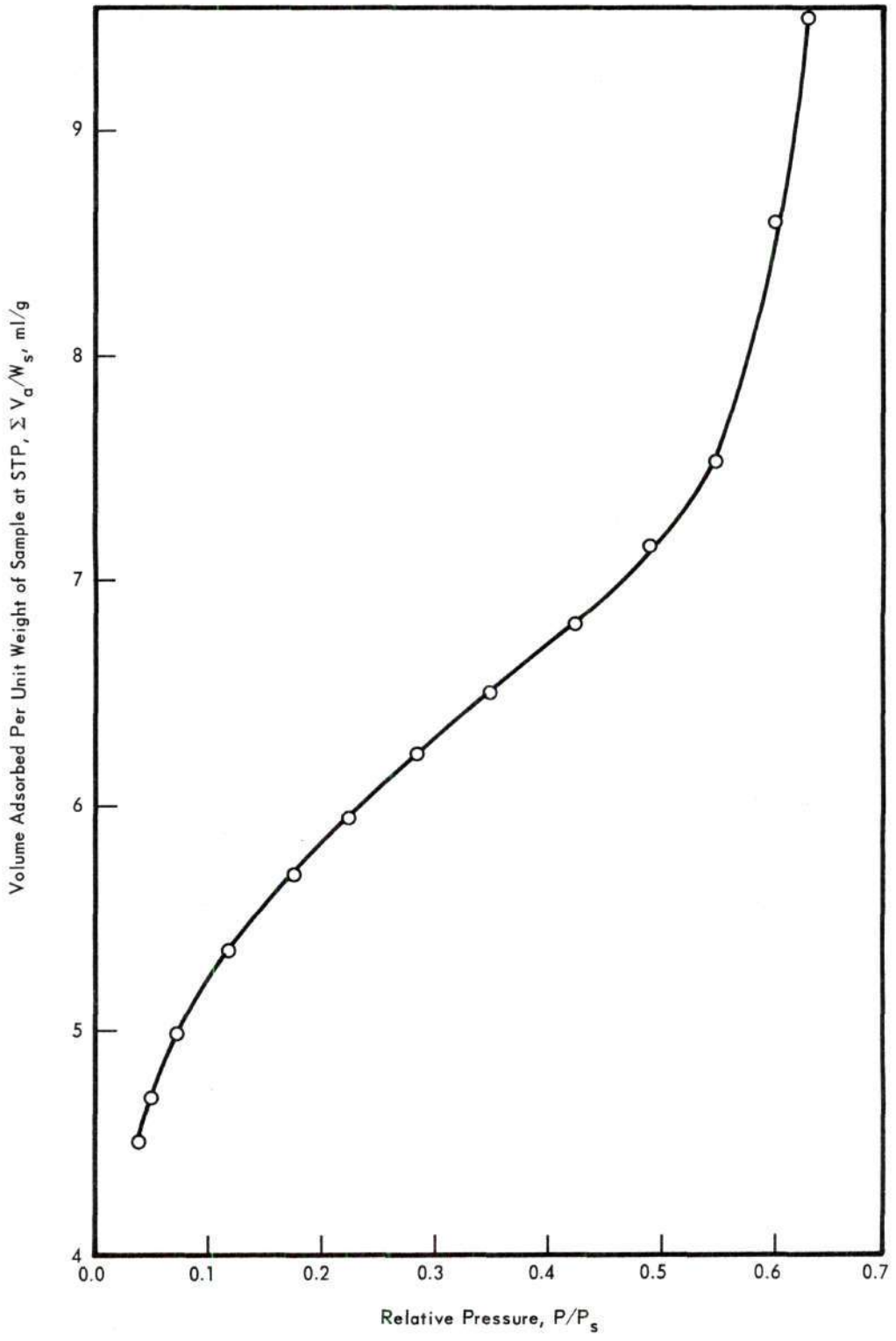

Figure 7. Krypton Desorption Isotherm for Boron Nitride Powder at 77.3 ^{o}K.

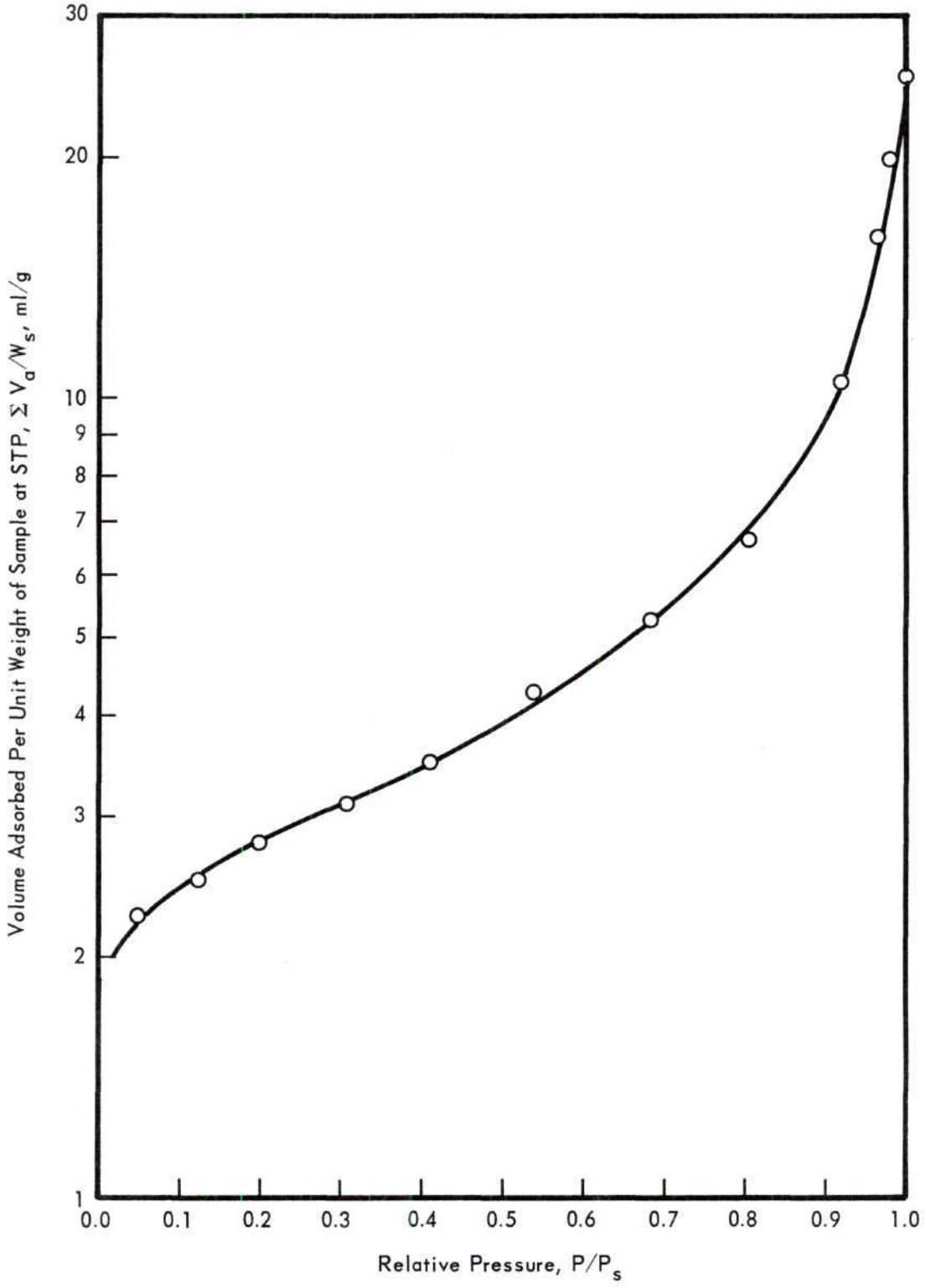

Figure 8. Nitrogen Desorption Isotherm for Kaolin Powder at 77.3 °K.

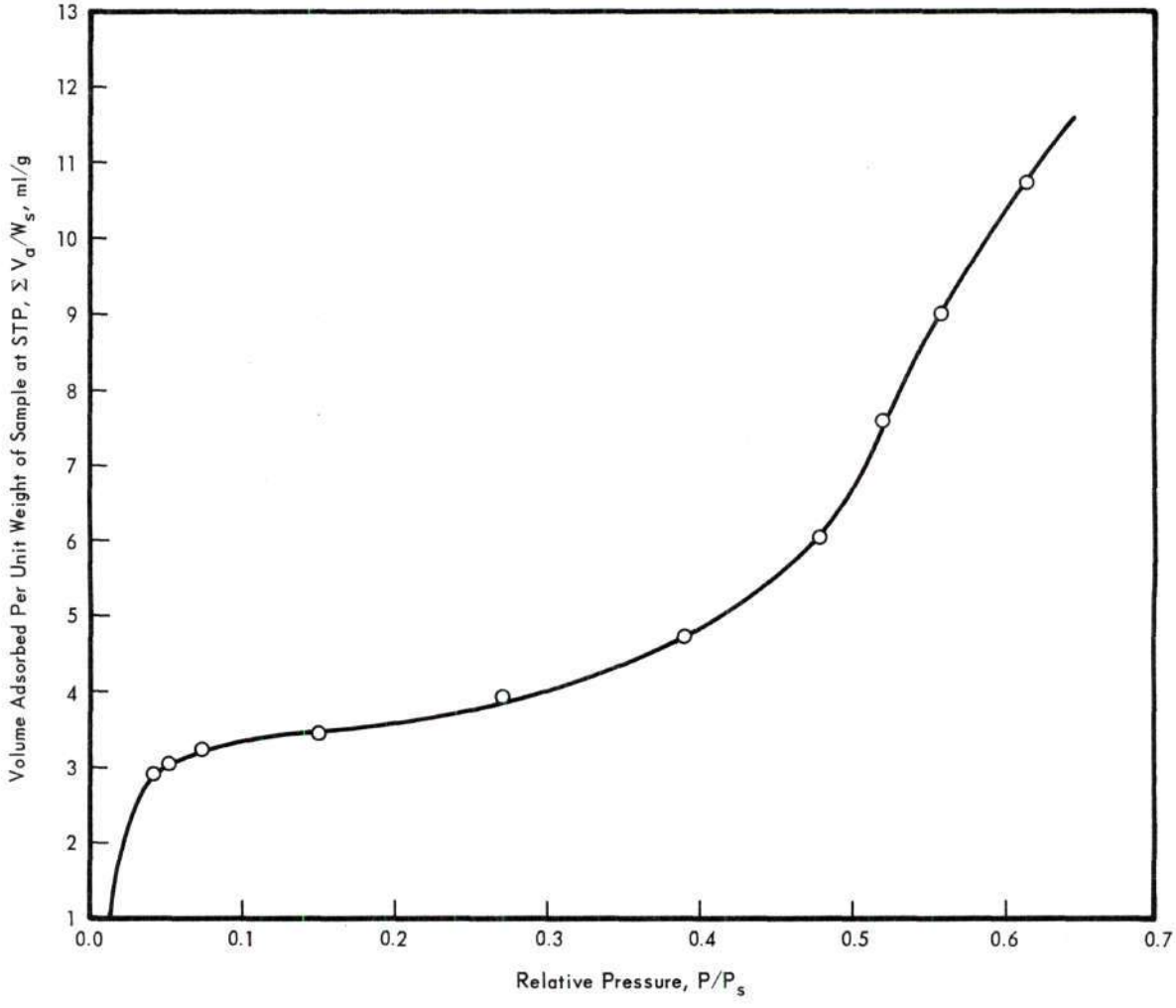

Figure 9. Krypton Desorption Isotherm for Kaolin Powder at 77.3 ^{o}K.

Table 2. Calculation Procedure for Pore Size Distribution.

1	2	3	4	5	6	7	8	9	10	11	12	13
P_2/P_s	$\Sigma(V_a/W_s)$	R	t	Δ (2)	(3)-(4)	Δ (4)	0.064(7)(12)	(5)-(8)	$\frac{(9)(3)^2}{(6)^2}$	$\frac{31.2\ (10)}{(3)}$	Σ (11)	$\frac{49600\ (10)}{(3)^2}$
	ml/gm STP	Å Units	Å Units	(ΔV)	(Rc-T)	(Δt)	(V_f)	(V_m)	(ΔV_p)	(ΔA_p)	(A_p)	(ΔL_p)

successive differences in the fourth column's values. The first entry position in the eighth column is blank and the second is zero; other positions cannot be filled until the computation is carried out for the first terms in columns nine, ten, eleven,and twelve. Column nine is the difference between the column five and the column eight values. Column ten is then derived from data in columns three, four, and nine. Column eleven is computed from column ten and column three data. Column twelve is the summation of column eleven. Column eight values for one determination are computed using column twelve values from the previous test. Once the first value in column twelve is obtained, the other computations can be completed by calculating values across the table. Column thirteen is calculated from columns nine and three.

By way of explanation of what has been accomplished upon completing this computation, column eight values give the quantity of gas in cubic centimeters per gram desorbed at STP. The pores actually were filled during the test with something that closely approximated a liquid,rather than a gas even though the results are given in terms of a gas volume. The liquid's volume and hence the true pore volume can then be obtained by multiplying the values in column ten by 0.001558 for N_2[3]. The corresponding value will be given for krypton in Chapter IV. Column eleven gives the surface area represented by all pores A_p of the radius given in column three. Column twelve entries represent the summation of surface area in m^2/gm that may be attributed to pores equal to or larger than the corresponding radius given in column three. Column thirteen gives the combined length of all pores L_p in millions of meters per gram of material of the corresponding radius indicated in column three. The pores are assumed to be cylindrical in these calculations.

CHAPTER IV

DISCUSSION OF RESULTS

Following the procedure described in Chapter III adsorption-desorption, isotherms for three different substances were evaluated at liquid nitrogen temperature. Both nitrogen and krypton gases were used as adsorbates. Figs. 4, 5, 6, 7, 8, and 9 show the desorption portions of the isotherms. In Appendix I data are given for the adsorption part. Surface areas were calculated both from the nitrogen and krypton data. The results for three adsorbents show differences of less than 2 per cent on the average.

The temperature varied from 77.36°K to 77.70°K for any one test. The nitrogen isotherms were evaluated to a relative pressure of 0.65. It is not possible to proceed beyond this point with krypton and the technique used. The relative pressure is calculated by dividing the actual pressure by the vapour pressure which liquid krypton would have at 77°K. This is below the triple point of krypton, however.

Many investigators have studied this triple point. Ziegler, Yarborough, and Mullins[23] select a value of 115.76°K. They report vapor pressures as shown in Table 3. At 77.36°K this would indicate a pressure of about 1.74 mm whereas the value extrapolated from liquid data is 2.49 mm.

Possibly, krypton adsorbed on a surface at 77°K behaves like a liquid, but a pressure higher than 1.74 mm cannot be reached because

Table 3. Krypton Vapor Pressure Extrapolated from Liquid Data

Temperature, ^{o}K	Vapor Pressure, mm Hg
77^{o}	1.607
78	2.013
79	2.507
80	3.104
81	3.824
82	4.686

krypton is crystallizing about the sample on the wall of the sample tube; this happens before it can be adsorbed as another adsorbate layer on the krypton already on the sample surface. At about 0.65 relative pressure there thus occurs what appears to be unlimited adsorption because of this crystallization or sublimitation.

The pore size distributions were calculated from the nitrogen isotherms following the procedure described in Chapter III using the values for film thickness and critical pore radius as given in Table 4. For krypton, however, the density at the working temperature in the adsorbed phase has to be evaluated before values of film thickness and critical pore radius can be assigned. Cook[11] gives density data for krypton as shown in Fig. 10 at the saturation pressure. A negligible error, probably, is introduced if these data are extrapolated to the temperature of interest here, assuming the change in the density from saturation to the actual pressure is negligible. The indicated value is 2.705 g/cm^3, and the molal volume is then 30.97 cm^3/mol. According to the method of calculation as indicated in Table 2, each gas volume at STP has to be converted into a liquid volume in order to find the volume occupied by the adsorbate, during the adsorption. Making the conversion with the above evaluated properties of krypton, the constants in column 8, 11, and 13, respectively, being 0.064, 31.2, and 49600 for nitrogen should be 0.072 27.5, and 42900 for krypton. According to the theory described in Chapter I, the intermolecular tension of krypton in the liquid phase absorbed on the powders has to be known at the working temperature. But there is no liquid krypton in existance, except probably molecular layers adsorbed on a surface. In order to estimate the surface tension

Table 4. Critical Pore Radius and Adsorbed Film Thickness for Nitrogen as a Function of Relative Pressure

Relative Pressure, P/P_s	Critical Pore Radius, Å	Film Thickness, Å
0.10	9.7	5.55
0.20	12.1	6.05
0.30	14.9	6.92
0.40	18.1	7.60
0.50	22.1	8.30
0.60	27.8	9.24
0.70	37.1	10.4
0.80	54.7	12.1
0.85	73.0	13.4
0.88	90.0	14.5
0.90	106.5	15.5
0.91	120.0	16.0
0.92	134.0	16.7
0.93	152.0	17.5
0.94	175.0	18.5
0.95	208.0	19.8
0.96	258.0	21.4
0.97	335.0	23.5
0.98	490	29.0
0.99	940	35.0

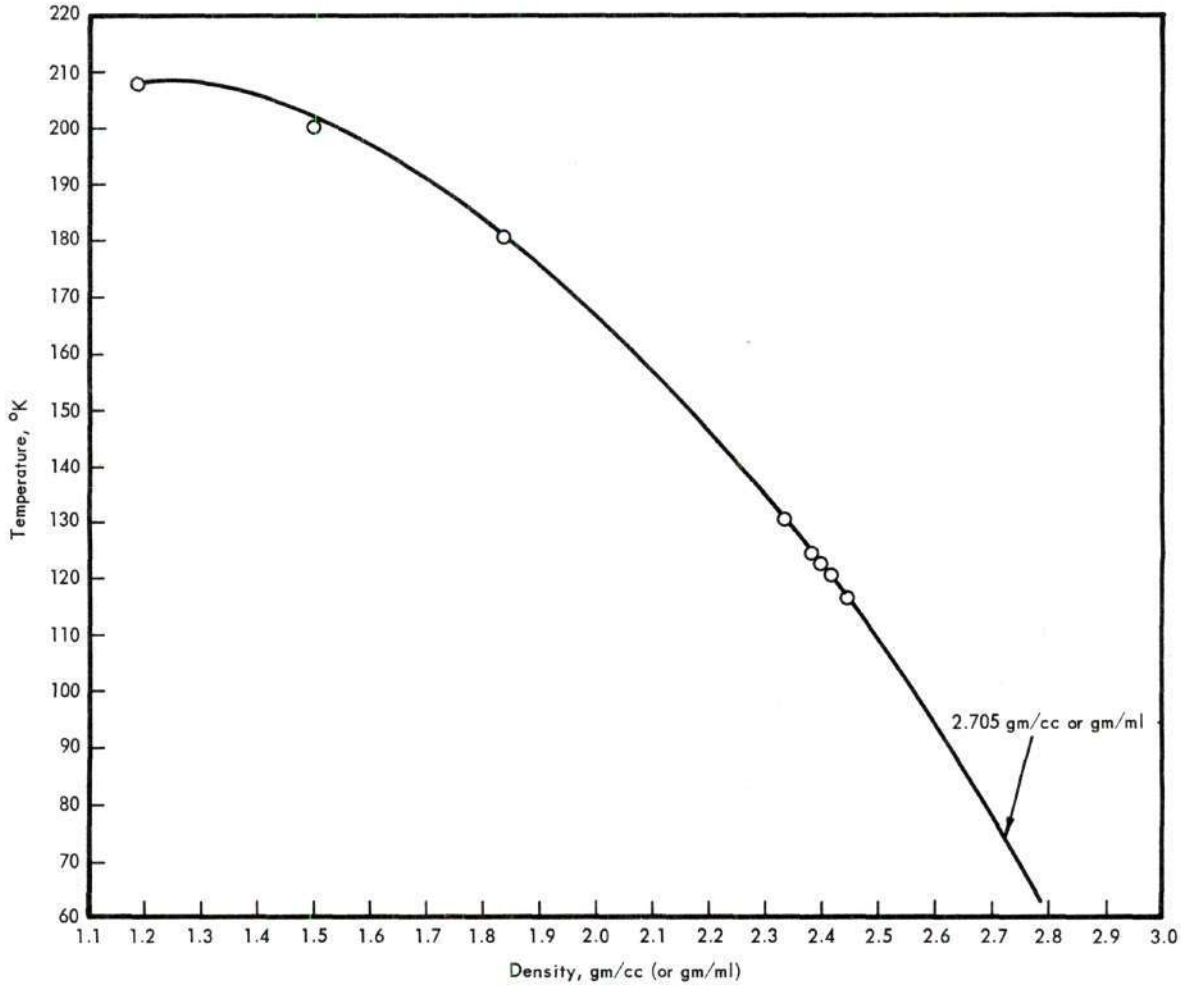

Figure 10. Density of Krypton versus Temperature at one Atmosphere.

σ of krypton, the law of corresponding states was used. This law applied to surface tension gives the result that $\sigma/(K\ T_c\ P_c^{\ 2})^{1/3}$ should be a universal function of T/T_c. Here K is the Boltzman constant and T_c and P_c are the critical temperature and pressure, respectively. Cook[11] gives data for argon as listed in Table 5; the same source indicates that T_c is 171°K and P_c is 48.3 atm. From these data, values of $\sigma/(K\ T_c\ P_c^{\ 2})^{1/3}$ are calculated and the results are plotted in Fig. 11. A surface tension of 22.0 dyne/cm^{-1} is then calculated for krypton, at 77°K using krypton critical constants which are 210°K and 54.3 atm. Because krypton and argon have similar properties, these results should be reliable.

The critical pore radius can then be calculated if the surface tension value is included. The film thickness of krypton has to be evaluated first. An equation analagous to Eq. (18) can be written assuming 4.5 Å for the molecular diameter of krypton. The result is

$$t(\text{Å}) = 4.5 \left[\frac{5}{\ln P/P_s} \right]^{1/3} . \qquad (26)$$

The radius of the meniscus r_m for krypton is then written using the Kelvin equation

$$R_g\ T \ln \frac{P}{P_s} = \frac{2\sigma v}{r_m} .$$

The final expression is $r_m = - \frac{2\sigma v}{R_g\ T \ln P/P_s}$. When this value is added to the film thickness the critical pore radius R_c is derived. In Table 6, R_c and t are given for different relative pressure at a temperature of 77.3 °K.

Table 5. Surface Tension of Argon Versus Temperature

Temperature, ^{o}K	Surface Tension, dyne cm^{-1}
85	13.12
90	11.86
100	9.42
110	7.10
120	4.95
130	2.99
140	1.28
145	0.57

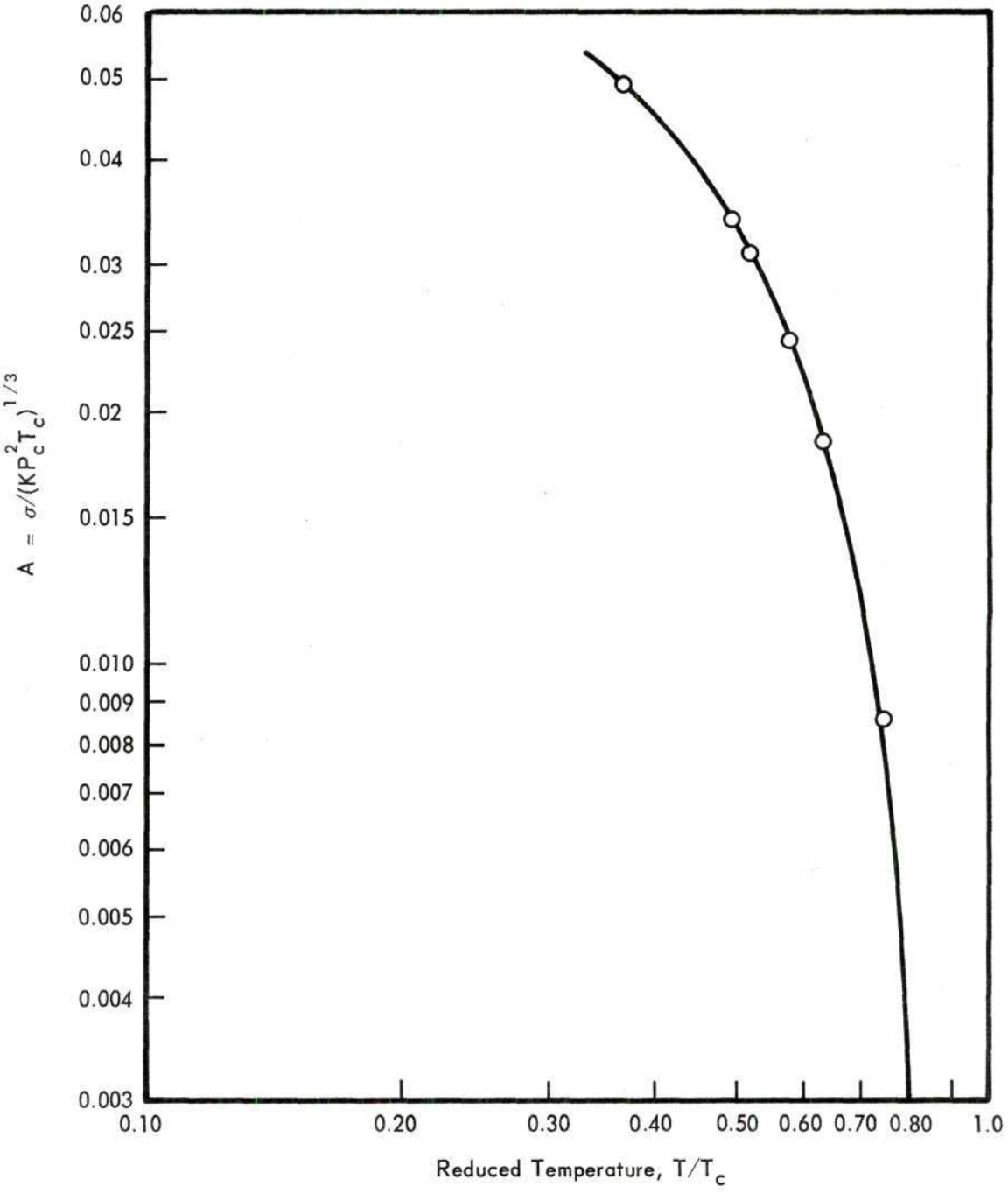

Figure 11. Dimensionless Group Plotted Against Reduced Temperature for Evaluating the Surface Tension of Krypton at 77.3 °K.

Table 6. Critical Pore Radius and Adsorbed Film Thickness as a Function of Relative Pressure.

Relative Pressure, P/P_s	Critical Pore Radius, Å	Film Thickness, Å
0.10	16.5	5.82
0.20	21.0	6.45
0.30	26.5	7.03
0.40	33.0	7.77
0.50	41.3	8.68
0.60	54.0	9.63
0.70	72.8	10.80
0.80	110.0	12.60
0.85	147.0	14.25
0.88	183.0	15.30
0.90	220.0	16.29
0.91	245.0	17.10
0.92	283.0	18.05

Calculations for krypton were then made as described for nitrogen with the above values utilized in columns 3 and 4 of the calculation sheet, Table 2. Column 1 and 2 values were derived reading very carefully the quantity adsorbed at the appropriate relative pressure from the desorption isotherms. As many points as possible were taken in order to secure small errors in the numerical integration; R_c and t were taken as average quantities. The results so obtained usually still showed a scattering due to inaccuracies in reading the isotherm. Therefore a least-squares calculation was made, fitting the values derived for krypton and for nitrogen between a critical pore radius of 20 and 50 Å. to an n-degree polynomial. Finally, the length of the pores of each certain radius was plotted against this radius. As mentioned before, the highest relative pressure attained with krypton was about 0.65. At this point, assuming the liquid state and equilibrium conditions, the pores with a radius of about 60 Å were filled. The other pores, or at least their surfaces were covered with a film. The question then arises how much surface is included in the pores filled and how much in the pores covered with a film of krypton. The last value has to be known in order to proceed with the calculations from column 12 on the calculation sheet. This column shows the pore surface which is covered with a film.

At the end of column 12 at a point where all surface is covered with the film (down to about 0.2 relative pressure), a value close to the surface area calculated from the desorption isotherm should be shown. This was the case for all the nitrogen calculations. However, for krypton the following modification was tried. A value for the surface

covered with a film at about 0.60 relative pressure (surface area of pores above 60 Å in radius) was assigned and then the calculation procedure executed. This was done with many different values in the first place of column 12, Table 2, and the last place was sought which would give a surface area comparable to that calculated from the adsorption isotherm.

These calculations were carried out on the Burroughs 220 digital computer since it was too tedious for hand computation. It showed that assigning a value for the first of column 12 led to even worse results and sometimes even gave an indication of negative pores. The best results were obtained assigning no number to the first place in column 12 and assuming the film thickness not to change very much in those pores not completely filled (i.e.,) no krypton desorption from this film. It then still is questionable whether the film was built up to the extent as predicted from Table 5 during the adsorption. For three different substances results are shown in Fig. 12. The pore size distributions show reasonable agreement with very different materials over the pore radius range 25 to 55 Å .

Below 25 Å the theory is not applicable due to the possibility of changes in density, surface tension, and other properties in very small capillaries. Krypton results (Fig. 12) were found to show poor agreement with nitrogen in this region.

Pore size calculations using data from the nitrogen desorption isotherm for aluminum powder show poor agreement with those of the krypton isotherm up to apparent pore radii of about 35 Å. It has to be taken into consideration that the total amount of nitrogen absorbed is small in these measurements, so experimental errors likely are involved. A

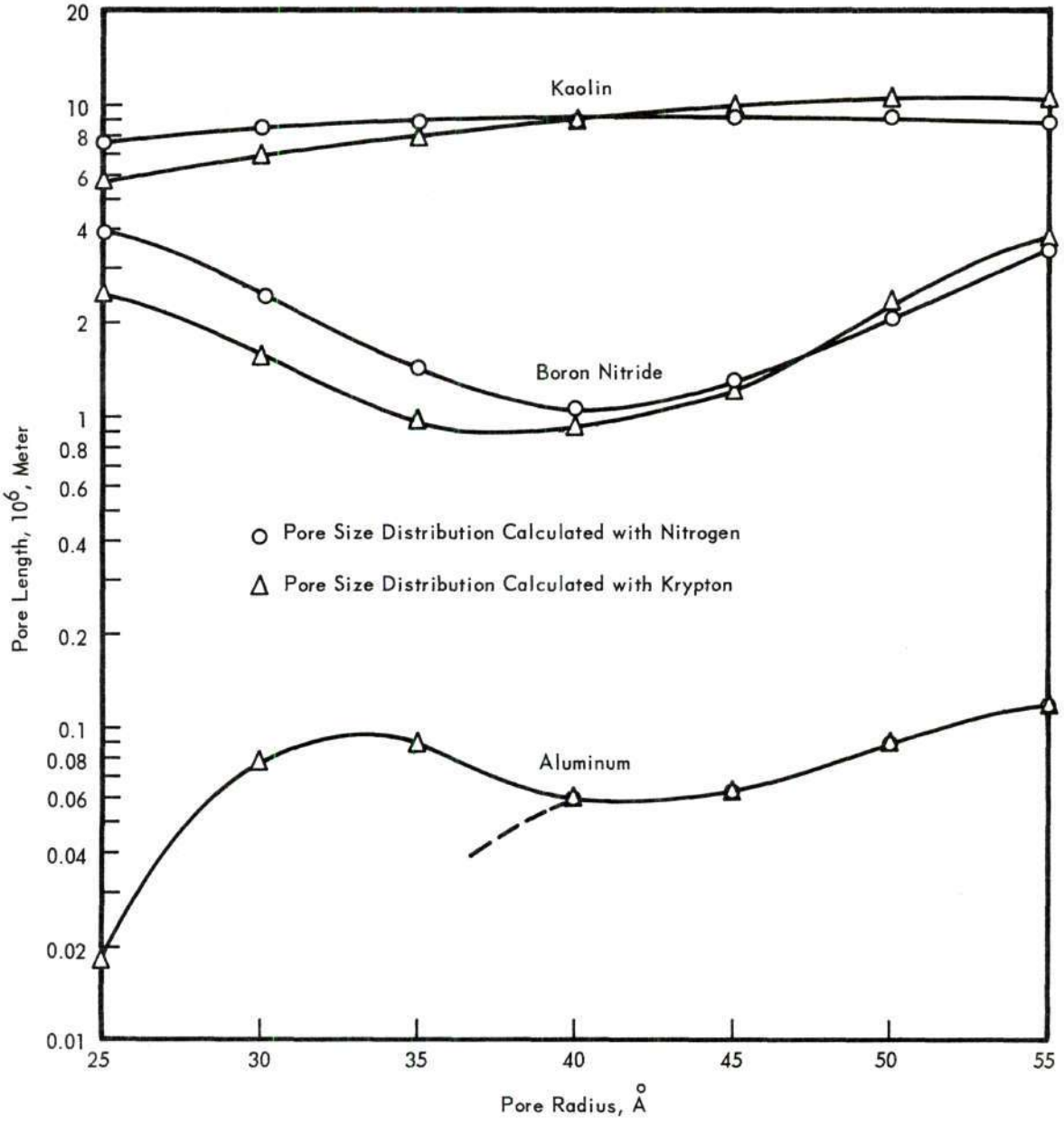

Figure 12. Pore Size Distributions Calculated with Nitrogen and Krypton.

precise determination of the desorption isotherm might be expected to yield somewhat better agreement.

Furthermore, boron nitride and aluminum powder adsorbed only a monolayer or slightly more up to 0.5 relative pressure. According to the Halsey model,[12] under such conditions film thickness increases in steps. These are rather large at the lower relative pressures. The equation used for the film thickness here is a smoothed form of the step model and might actually be inapplicable for boron nitride and aluminum powder. Both powders may well not be porous at all. What was measured then could have been the void spaces existing among the particles, especially near points of contact. These same spaces would have been determined with both the nitrogen and krypton. Hence, the results should be consistent one with the other. This is true for pores above about 35 Å in radius.

Kaolin is undoubtedly porous. Here both measurements are in good agreement.

CHAPTER 5

CONCLUSIONS

1. Krypton can be used in analyzing pore volume distributions with substances having pore radii between 25 to 60 Å as satisfactorily as can the nitrogen adsorption technique.

2. When the solid is not porous, void spaces among the particles are likely to give an indication of pores. The adsorption isotherm may afford a clue to the true condition in this case. If the isotherm shows little adsorption between relative pressures of about 0.2 to 0.7, this possibly indicated that voids and not pores are being indicated.

3. Use of liquid properties for krypton in the adsorbed phase at conditions below krypton's triple point gives results that compare favorably with those using nitrogen.

CHAPTER 6

RECOMMENDATIONS

An adsorbate having the following properties at a temperature near $77^{\circ}K$ would be best for measuring pore structure of low-porosity materials by the low-temperature desorption method:

(1) A low saturation pressure. This makes the working pressure low throughout the isotherm and because of this, volume changes can be measured accurately. The saturation pressure should be of the order of 2 mm of Hg, because at lower pressures errors arise in the pressure measuring devices and then the slightest leak gives erroneous data.

(2) A small molecular diameter. This makes it easy for the molecule to enter a pore and makes possible measuring smaller pores with greater precisions.

(3) A triple point above the working temperature. This will assure condensation as a liquid up to the saturation pressure.

(4) Inertness. This will avoid complications due to chemisorption.

(5) Obtainable in a pure form.

When all these considerations are taken into account, ethane at about $-260^{\circ}F$ appears to be best. This temperature could then be obtained with an organic liquid-solid mixture which has its melting point at about this temperature such as dichlorodifluormethane or isopentane. These compounds could then be cooled to a solid by means of liquid nitrogen.

Another possibility is increasing the vapor pressure above liquid nitrogen. The desired temperature in the nitrogen cooling liquid exists at about 15 atmosphere pressure.

APPENDIX

Adsorption data for both nitrogen and krypton and surface areas calculated for three different substances.

Table 7. Krypton Adsorbed on Kaolin Powder at 77.36°K

Relative Pressure	Gas Adsorbed per Unit Sample Weight, ml/gm at STP	$\frac{P_2/P_s}{(1-P_1/P_s\ VA/W_s)}$
0.001	0.309	0.0038
0.016	0.665	0.0245
0.078	1.203	0.0706
0.184	2.755	--
0.325	3.250	--
0.444	4.703	--
0.522	6.181	--
0.602	9.817	--

Calculated Surface Area, 7.42 m^2/g.

Table 8. Nitrogen Adsorbed on Kaolin Powder at 77.36°K

Relative Pressure P_2/P_s	Gas Adsorbed per Unit Sample Weight ml/gm at STP	$\frac{P_2/P_s}{(1-P_2/P_s)\ V_a/W_s}$
0.099	2.023	0.0545
0.203	2.337	0.1096
0.302	2.565	0.1693
0.422	3.006	0.2431
0.563	3.767	--
0.710	4.695	--
0.853	6.882	--
0.958	12.60	--
1.000	25.11	--

Calculate Surface Area, 7.50 m^2/g.

Table 9. Krypton Adsorbed on Boron Nitride at 77.36°K

Relative Pressure P_2/P_s	Gas Adsorbed per Unit Sample Weight ml/gm at STP	$\frac{P_2/P_s}{(1-P_2/P_s)\ V_a/W_s)}$
0.050	2.615	0.0201
0.106	3.202	0.0371
0.150	3.593	0.0493
0.206	3.967	0.0655
0.273	4.263	0.0881
0.334	4.747	--
0.381	5.498	--
0.461	6.480	--
0.554	7.549	--
0.600	8.615	--
0.630	9.516	--

Calculated Surface Area, 18.30 m^2/g.

Table 10. Nitrogen Adsorbed on Boron Nitride at 77.36°K

Relative Pressure P_2/P_s	Gas Adsorbed per Unit Sample Weight, ml/gm at STP	$\frac{P_2/P_s}{(1-P_1/P_s\ V_a/W_s)}$
0.008	2.863	0.0029
0.067	3.971	0.0181
0.151	4.669	0.0381
0.245	5.318	0.0613
0.346	6.210	--
0.455	7.150	--
0.568	8.166	--
0.676	9.932	--
0.762	11.91	--
0.800	12.85	--
0.890	18.00	--
0.928	24.20	--
0.949	31.46	--
0.979	61.88	--
0.990	83.16	--

Calculated Surface Area, 18.40 m^3/g.

Table 11. Krypton Adsorbed on Aluminum Powder 77.36°K

Relative Pressure P_2/P_s	Gas Adsorbed per Unit Sample Weight, ml/gm at STP	$\frac{P_2/P_s}{(1-P_2/P_s)\ V_a/W_s}$
0.001	0.151	0.0930
0.070	0.189	0.3980
0.077	0.200	0.4184
0.108	0.214	0.5661
0.152	0.232	0.7761
0.214	0.248	--
0.285	0.272	--
0.361	0.292	--
0.421	0.320	--
0.481	0.351	--
0.534	0.375	--
0.566	0.401	--
0.662	0.409	--
0.682	0.462	--

Calculated Surface Area, 1.18 m^2/g.

Table 12. Nitrogen Adsorbed on Aluminum Powder at 77.70°K

Relative Pressure P_2/P_s	Gas Absorbed per Unit Sample Weight, ml/gm at STP	$\frac{P_2/P_s}{(1-P_2/P_s)\ V_a/W_s)}$
0.090	0.270	0.3679
0.191	0.326	0.7269
0.292	0.366	0.1127
0.399	0.408	0.1630
0.513	0.482	--
0.634	0.599	--
0.775	0.857	--
0.917	2.984	--
0.968	7.042	--
0.982	11.38	--
0.992	16.79	--

Calculate Surface Area, 1.21 m^2/g.

BIBLIOGRAPHY*

1. S. Brunauer, L.S. Deming, W.E. Deming, and E. Teller, "On a Theory of the Van der Waals Adsorption of Gases," J. Amer. Chem. Soc., 62, 1723-32 (1940).

2. D.M. Young and A.D. Crowell, "Physical Adsorption of Gases", (Butterworth's, Washington, 1962).

3. J.D. Gilchristand, and J. Taylor, "Macro Pore Size Analysis of Metallurgical Coke," J. Inst. Fuel, 24, 207-11 (1951).

4. C. Orr, Jr., and J.M. DallaValle, "Fine Particle Measurement," (The Macmillan Co., New York, 1959).

5. L.C. Ritter, and R.L. Drake, "Pore Size Distribution of Porous Materials," Ind. Eng. Chem., Anal. Ed. 17, 782-6 (1945).

6. J. Briscol and B.E. Warren, "An X-ray Study of Carbon Black," J. Appl. Phys., 13, 364-71 (1942).

7. M.H. Jellinek and I. Frankuchen, "X-ray Diffraction Examination of Gamma Aluminum," Ind. Eng. Chem. 37, 158-63 (1945).

8. G. Fournet and A. Guinier, "The Present State of the Theory of Low Angle Scattering of X-rays," J. Phys. Radium II, 516-520 (1950).

9. S. Ergun, "Determination of Particle Density of Crushed Porous Solids," Anal. Chem. 23, 151-6 (1951).

10. S. Ergun, "Precision Measurements of Gas Flow Rates," Anal. Chem. 25, 1222-6 (1953).

11. G.A. Cook, "Argon, Helium and the Rare Gases," Vol I., (Interscience Publishing Co., New York, 1961).

12. A. Wheeler, "Reaction Rates and Selectivity in Catalyst Pores," Catalysis, Vol. II, (P.H. Emmet, ed., Reinhold Publ. Co., New York 1955).

13. W.O. Mulligan and C.R. Adams, "An Analytical Expression for Cumulative Pore Volume and Pore Size Distributions," J. Phys. Chem. 58, 891-3 (1954).

14. E.M. Voight and R.H. Tomlinson, "The Determination of Pore Size Distribution and Surface Area from Adsorption Isotherms," Can. J. Chem. 33, 215-231 (1955).